Mobile Integrons Encode Phage Defense Systems

Nicolas KIEFFER[1,2♦], Alberto HIPÓLITO[1,2♦], Paula BLANCO[1,2], Thomas DELOBELLE[3], Laura ORTIZ-MIRAVALLES, Francisco Manuel OJEDA[1,2], Thomas JOVÉ[4], Dukas JURENAS[3], Meritxell GARCÍA-QUINTANILLA[5,6], Pilar DOMINGO-CALAP[7], José Antonio ESCUDERO[1,2*]

[1]Molecular basis of Adaptation Laboratory, Departamento de Sanidad Animal, Facultad de Veterinaria de la Universidad Complutense de Madrid, Madrid, España,
[2]VISAVET Health Surveillance Centre, Universidad Complutense de Madrid, Spain.
[3] Laboratoire de Génétique et Physiologie Bactérienne, Faculté de Sciences, Université Libre de Bruxelles (ULB), Gosselies, Belgium.
[4]INSERM, CHU Limoges, RESINFIT, University of Limoges, Limoges, France, Present address: no longer employed by INSERM.
[5]Departamento de Microbiología, Instituto de Investigación Sanitaria Fundación Jiménez Díaz, Madrid, España
[6]CIBERINFEC-CIBER de Enfermedades Infecciosas, Instituto de Salud Carlos III, Madrid, Spain
[7]Instituto de Biología Integrativa de Sistemas, Universitat de València-CSIC, Paterna, Spain.

♦Both authors contributed equally

*Corresponding Author. Email: jaescude@ucm.es
+34 661584761
University Complutense of Madrid,
Department of Animal Health,
Avenida Puerta de Hierro s/n
28040, Madrid, Spain.

ABSTRACT

Integrons are bacterial genetic elements that capture, stockpile and modulate the expression of genes encoded in integron cassettes. Mobile Integrons (MI) are borne on plasmids, acting as a vehicle for hundreds of antimicrobial resistance genes among key pathogens. These elements also carry gene cassettes of unknown function (*gcu*s) whose role and adaptive value remains unexplored. Recent years have witnessed the discovery of a myriad defense systems against bacteriophages, highlighting that viral infection is a major selective pressure for bacteria. We hence sought to explore if *gcu*s could encode phage defense systems. Using the INTEGRALL database, we established a collection of 129 *gcu*s in pMBA, a vector where cassettes are established as part of a class 1 integron. PADLOC and DefenseFinder predicted four phage defense systems in this collection, comprising Lamassu, CBASS and two ABI (abortive infection) systems. We experimentally challenged all cassettes with phages and found eleven additional candidates that were not detected *in silico*. We have characterized in depth the 15 *gcu*s against a panel of phages in *Escherichia coli* confirming their role as phage defense integron cassettes (PICs). We used recombination assays to verify that these are *bona fide* integron cassettes and are therefore mobile. We show that PICs confer resistance in other clinically relevant species, such as *Klebsiella pneumoniae* and *Pseudomonas aeruginosa.* Several PICs also limit prophage activation, providing protection at the population-level. Given the stockpiling capacity of integrons, we explored the additivity of phenotypes and found that integrons with two PICs confer multiphage-resistance. Additionally, when combined with antimicrobial resistance genes, integrons confer simultaneously drug and phage resistance. Crucially, we also show that the position of a *pic* in the array can strongly decrease its cost. Our results prove a role of integrons in phage defense, acting as highly mobile, low-cost defense islands.

INTRODUCTION

Antimicrobial resistance (AMR) is a major public health concern worldwide, and the emergence of multi-drug (MDR) resistant bacteria is making increasingly difficult to treat infections with antibiotics[1]. Alternative therapeutic options are being explored as potential solutions to this problem. Phage therapy -the use of viruses that infect and kill bacteria- is an old approach (it predates the use of antibiotics) that is currently being revisited and building momentum. Several recent reports have yielded positive results for the treatment of life-threatening infections caused by MDR bacteria[2–4]. However, the efficacy of phage therapy can be limited by the emergence of phage-resistant bacteria[5,6]. Resistance can typically emerge through mutations in which the receptors recognized by the phage are lost, or through the acquisition of defense systems. In recent years, a plethora of new defense systems have been discovered and characterized to varying extents, adding to the classic restriction-modification enzymes or the more recently discovered CRISPR-Cas immune systems[7]. These can be classified according to the mechanism used to sense phage infection into systems that detect nucleic acids, phage proteins, the integrity of the host, and others[8,9]. These defense mechanisms have evolved in response to phage predation, and they are often encoded in the vicinity of other systems, creating defense islands. In fact, it was the proximity to known defense systems that allowed the initial discovery of systems such as Lammasu, Kiwa, Thoeris, or Zorya, using a guilt-by-association rationale[9–11]. Ever since, we have witnessed a sheer increase in the discovery of novel defense systems. Their abundance in genomes illustrates the ongoing evolutionary arms race between bacteria and their phages and highlights the importance of phage predation as a selective pressure for bacteria[12]. Defense systems have been shown to be encoded in mobile genetic elements such as integrative conjugative elements, transposons, or prophages[12]. However, they are proven to impact the fitness of the bacterial strains carrying them due to the constitutive expression of their genetic content[13] highlighting the cost of resistance.

Integrons are genetic elements that play an important role in bacterial adaptation to changing environmental conditions[14–16]. They capture and accumulate new genes embedded in integron cassettes (ICs), acting as genetic memories of adaptive functions[17]. Integrons typically consist of a conserved platform encoding the integrase gene and the recombination site in the integron (*attI*)[18]; and a variable region containing the cassettes. Cassettes are incorporated into the *attI* site through site-specific recombination reactions mediated by the integrase and are expressed from the dedicated Pc promoter encoded in the platform[19]. The integrase can also reorder cassettes in the array to modulate their expression, modifying their distance to the Pc

and the polar effects they are subjected to[20–22]. The expression of the integrase is controlled by the SOS response, so that integrons provide to their hosts "adaptation on demand"[23,24].

Mobile integrons (MI) are a subset of integrons that are typically associated with mobile genetic elements, such as plasmids and transposons, which can facilitate their horizontal transfer between bacterial cells[25–27]. They are a palpable example of the evolvability these platforms confer to their hosts. They were initially discovered in the first MDR isolates of *Shigella* spp. during the 1950's, carrying two resistance genes[16,28]. Nowadays MIs are commonplace among key Gram-negative pathogens[29] carrying almost 200 resistance genes against most antibiotic families[30–32]. Consequently, MIs are generally considered to be devoted almost exclusively to AMR. Nevertheless, among the cassettes found within MIs are gene cassettes of unknown function (*gcu*) whose importance has generally been overlooked. Yet the working model of integrons suggests that cassettes must be adaptive at the time of integration when they are expressed at the maximum strength[23]. We hence reasoned that *gcu*s could be playing an unknown adaptive role. Given the importance of phage predation in the lifestyle of bacteria and in their genome's content, we sought to explore the possibility that *gcus* encode phage defense systems.

Here we have selected 129 *gcus* from the INTEGRALL database[33], and cloned them in pMBA, a plasmid mimicking the genetic environment of a mobile integron[32]. DefenseFinder[34] and PADLOC[35] predicted 4 *gcus* in this collection as potential defense systems. We then used *in vitro* screening test with phages T4 and T7 combined with structural prediction using AlphaFold and discovered 9 novel defense systems that were not predicted. All cassettes confer resistance to at least one of a panel of 8 phages against *E. coli*. We have confirmed that all systems are encoded in *bona fide* (functional) integron cassettes, which we have named Phage defense Integron Cassettes (PICs). They are hence mobile and likely to circulate among other species. Indeed, we demonstrate that they also confer resistance in *K. pneumoniae* and *P. aeruginosa,* major pathogens of the ESKAPEE group. As part of an integron, cassettes can be stockpiled in an array. Building arrays, we show that the position of a PIC in the array can strongly diminish its cost and its function. We also show that phenotypes encoded in PICs are additive, conferring multi-phage or phage/drug resistance if combined with other PICs or antimicrobial resistance cassettes (ARCs). An update in DefenseFinder allowed to discover a novel defence system in an array with *pic24*, confirming that multiphage resistance integrons are already present in clinical isolates. Altogether, our work proves the involvement of integrons in phage defense, acting as repositories of a broad variety of defense systems i.e.: as mobile and low-cost defense islands.

129 **RESULTS**

130 **Integron *gcus* contain predicted phage defense systems.**

131 To obtain a broad set of *gcu*s in MIs we screened the INTEGRALL database, the largest
132 repository for mobile integron-related data (date: November 2021). We retrieved 303 cassettes
133 annotated as *gcu*s (< 95% nucleotide identity) with sizes ranging from 191 bp to 3 kb. We
134 further analysed and curated this list manually using BLAST. We discarded several cassettes
135 misannotated as *gcu*s in which an insertion sequence had interrupted a cassette of known
136 function. Additionally, gene-less cassettes -that failed to produce hits with any known or
137 unknown protein- were also discarded. We therefore selected a panel of 129 elements with sizes
138 ranging from 284 to 2.950 bp (Figure S1). All elements were synthesized *in vitro* and cloned in
139 pMBA, a vector providing a biologically sound genetic environment, where cassettes are
140 inserted in first position of a class 1 integron and are under the control of a strong Pc promoter
141 (PcS)[32]. The sequences of our selected collection were submitted in May 2022 to the two major
142 web platforms specialized in phage resistance gene prediction, DefenseFinder and
143 PADLOC[34,35]. As a result of this computational analysis, we identified four distinct gene
144 cassettes (*gcu*s 59, 128, 135 and N) as potential defense mechanisms, each exhibiting homology
145 to a known system involved in phage resistance (Figure 1A).

146 Given their newly identified putative function as phage resistance elements, we propose
147 to rename these *gcus* as *pic*s, while conserving their initial name for simplicity. Pic59 (formerly
148 Gcu59) was identified as a homolog of the AriAB system[36] and is suggested to confer phage
149 resistance through abortive infection. *pic128* encodes two ORFs (*pic128A* and *pic128B*) and
150 shows similarity to a Lamassu Type 1 system. AlphaFold predicts that Pic128A shares motifs
151 with YfjL-like or AbpA proteins, which are involved in phage defense, while Pic128B contains
152 a putative exonuclease domain. Interestingly, the three-dimensional structure of Pic128B
153 protein displays a remarkable similarity to DdmC, a protein from the Lamassu Type 2 plasmid
154 and phage defense system described in *Vibrio cholerae*[37]. *pic135* also contains two ORFs and
155 share structural similarity with a CBASS Type 1 system[38]. The proteins encoded by this cassette,
156 Pic135A and Pic135B, are predicted to play roles in nucleotidyl-transfer and membrane
157 translocation, respectively, as suggested by protein structure predictions. Last, PicN is
158 annotated as an AbiV family protein[39], implicated in phage resistance through abortive infection
159 mechanisms.

160

161

162

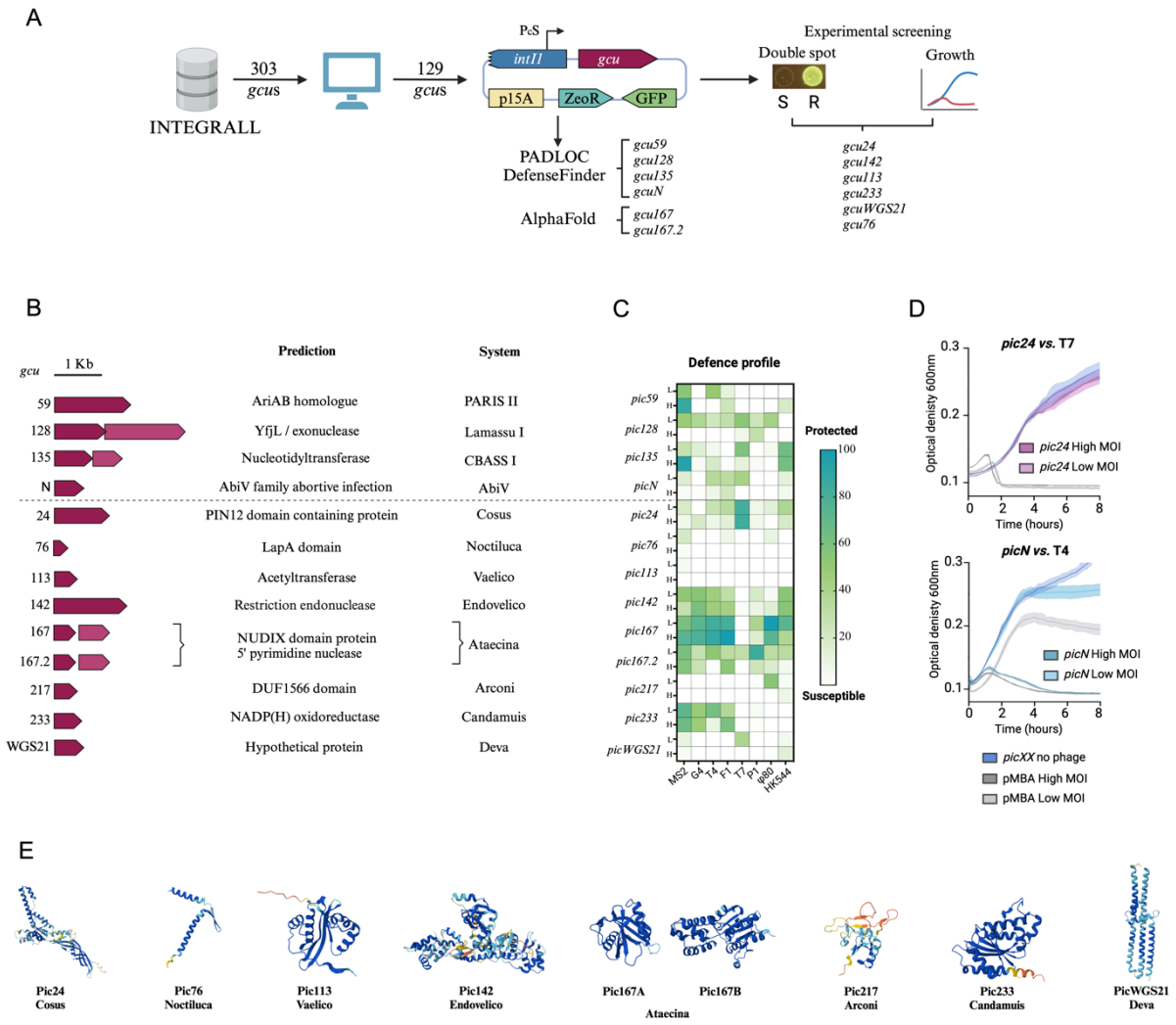

Figure 1. Identification and Characterization of Phage Defense Systems in Integron Cassettes. (A) Schematic workflow for the identification and experimental validation of phage defense systems in *gcus*. A collection of 303 gcus was extracted from the INTEGRALL database, curated to 129 *gcus*, and cloned into the pMBA vector, placing each *gcu* under the control of a strong integron promoter (PcS). Predicted phage defense systems were identified using PADLOC and DefenseFinder, (May 2022) and experimental screening was performed using a double-spot assay or growth curves to determine susceptibility or resistance to phage infection. **(B)** Genetic organization and predicted functions of selected *gcus*. Predicted function is shown for putative defense mechanisms and other candidate *gcus*. **(C)** Heatmap showing the defense profiles of identified Phage Integron Cassettes (PICs) against a panel of eight *E. coli* phages. The degree of protection (resistance) is indicated by the color scale, with dark green representing high protection, light green representing low protection, and white no protection. **(D)** Examples of growth curves used to build the heatmap in C: *pic24* confers strong resistance to phage T7 at both high and low MOI while *picN* shows resistance to phage T4 only at low MOI. Growth curves are represented as the mean of three independent replicates. The standard error of the mean is represented as a lighter colour shade. **(E)** Structure of novel phage defense systems, as predicted by AlphaFold2.

Functional screening and domain prediction reveal additional phage defense systems.

Bioinformatic approaches can fail to detect novel systems that are not similar to any of the known ones. We hence turned to *in vitro* experiments to detect novel resistance mechanisms within our *gcu* collection. We employed a double spot screening protocol in solid media and the monitoring of growth curves in liquid media, to challenge the whole collection with different

concentrations of phages T4 or T7 (Figure 1A and Figure S2). We successfully detected 7 new candidates (*pic24, pic142*, *pic233, pic217, pic113, picWGS21* and *pic76*) presenting substantial growth in the presence of phage (Figure S2). Using AlphaFold prediction model to find proteins with potential nuclease domains, that are often linked to phage defense, we additionally identified *pic167* and its close homolog *pic167.2*. *in silico* structural predictions of proteins encoded in these PICs suggest a diversity of functional roles. Both Pic167 and Pic167.2 are likely involved in nucleotide metabolism, with indications of NUDIX hydrolase and nucleotidase activities. Pic142 is a putative restriction endonuclease, while Pic24 possesses a PIN12 domain that potentially acts as a nuclease[40]. Pic233 is possibly a NADP(H) oxidoreductase; Pic113 is a putative GNAT N-acetyltransferase and Pic217 a putative integral membrane protein with a lectin C domain. AlphaFold did yield relevant homologs with a known function for PicWGS21. Last, Pic76 is a small protein of 76 amino acid that contains a LapA domain that has been related to biofilm formation[41] (Figure 1B). To adhere to the custom in the field, these novel systems are also given the name of a deity of Celtiberian mythology (Figure 1B).

PICs confer protection to a panel of phages *Escherichia coli.*

To characterize in depth the role and profile of PICs in phage resistance, we subcloned the whole library in strain *E. coli* IJ1862 (an F' strain that can be infected by plasmids targeting the conjugative pilus[42]) and conducted infection assays with a panel of phages from different families at varying multiplicities of infection (MOIs). We monitored the optical densities (OD_{600}) over time of bacterial cultures in presence and absence of phage MS2, F1, G4, T4, T7, P1, Φ80 and HK544. As a control, we included an isogenic strain carrying the empty vector pMBA. We used the area under the (growth) curve to determine the protective effect of the cassette, as in[43] (see Materials and Methods). Our data showed that all PICs conferred resistance to at least one condition (one phage at one MOI) (Figure 1C and Figure S3), confirming their role in phage defense. Resistance profiles were diverse, with some PICs showing broad-spectrum resistance, such as *pic167, pic167.2*, *pic128* and *pic142*. Others, as *pic24,* showed a narrower spectrum with low level resistance against several phages, but very high resistance against phage T7 at both high and low MOI (Figure 1D). The resistance phenotype displayed by *picN*, limited to low MOI for phages MS2, T4, F1 and T7, aligns with the characteristic phenotype of an abortive infection, thereby confirming the predictions made by PADLOC and DefenseFinder. Overall, our results confirm that the *gcus* identified in our screenings are indeed phage resistance genes with known and characterized mechanisms.

215

216 **PICs are *bona fide* integron cassettes.**

217 Identification of integrons and their cassettes has not been a straightforward task until
218 the appearance of IntegronFinder[44]. A large part of the content in INTEGRALL predates
219 IntegronFinder, so their classification as integron cassettes needs to be verified. A close analysis
220 of the genetic context, locating integrases in close vicinity and in opposite orientation, can be
221 indirect proof that a gene is indeed a cassette. Most PICs identified here -except for *pic135* and
222 *pic142*- are located within class 1 or class 2 integrons, often in pathogenic strains belonging to
223 the *Enterobacteriaceae* family (like *pic217*, *pic113*, and *pic24*) or multidrug resistant *P.*
224 *aeruginosa.* A compelling example of the latter is the presence of *picN* next to cassettes $bla_{IMP,}$
225 *aacA4* and *catB6,* conferring multidrug resistance to carbapenems, aminoglycosides, and
226 chloramphenicol, respectively (Accession number: AJ223604) (Figure 2A). Yet, given that
227 finding defense systems in integrons has important implications for the mobility of these
228 systems, we sought to verify experimentally that these are *bona fide* integron cassettes. Cassette
229 recombination is a site-specific reaction that can be evidenced in a suicide conjugation assay
230 that is typical in the field[16,45]. Crucially, recombination is semiconservative, involving the
231 bottom strand (but not the top strand) of both the *attC* sites in cassettes and *attI* sites of integrons
232 [46,47]. This unique feature can be easily detected because it leads to clear differences in the suicide
233 conjugation assay when the plasmid transfers the bottom or top strand of the cassette[47]. With
234 this in mind, we inserted the putative *attC* sites of all *pics* in both orientations in the suicide
235 vector pSW23T and measured the recombination frequency of both strands for each cassette.
236 Recombination events were verified through PCR. As expected, we observed a clear drop
237 (between 100- and 10.000-fold lower) in the recombination frequency of the top strands of all
238 putative *attC* sites, as would be expected from integron cassettes (Figure 2B). *picWGS21* had
239 extremely low recombination frequencies for the bottom strand. Yet recombination of the top
240 strand was only observed in 1 out of 6 replicate experiments, suggesting that it is indeed an
241 integron cassette albeit with a very poor recombination site. Indeed, the folded *attC* site of
242 *picWGS21* has the typical hairpin structure and extra-helical bases of these sites (Figure S4)[47–
243 49]. Hence, our data confirms that PICs are *bona fide* integron cassettes.

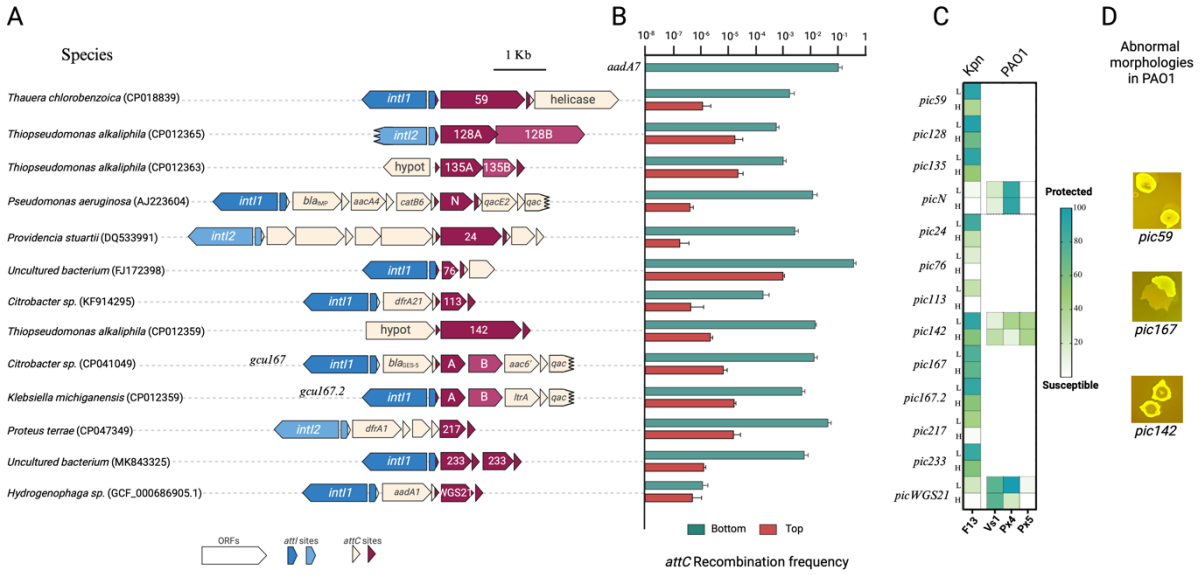

Figure 2. Genetic Context, Recombination Frequency, and Phage Protection Profiles of Identified PICs in other species. (A) Genetic context of PICs as found in databases, highlighting their association with integron integrases (*intI1* or *intI2*, in blue shades). PICs are found in different host species. Each PIC is annotated with its respective identifier (e.g., 59, 128A/B, 135A/B), along with known associated genes such as resistance genes (e.g., bla_{IMP}, *aacA4*, *catB6*). **(B)** Recombination frequency of the *attC* sites of the identified PICs. The recombination frequency was measured for the bottom (green bars) and top (red bars) strands of the *attC* sites using a suicide conjugation assay. Bars represent the mean of at least 3 biological replicates. Error bars correspond to the standard error of the mean. **(C)** Heatmap showing the protection profiles of PICs against phage infection in different host species, including *K. pneumoniae* (KP5) and *P. aeruginosa* (PAO1) against a panel of cognate phages (F13, Vs1, Px4, Px5).

Defense cassettes are protective in other species.

Given the mobility of integrons and cassettes among important pathogens, we sought to determine if PICs are active in different hosts. To this end, we evaluated the protective effects of PICs in *K. pneumoniae* and *P. aeruginosa,* two species of the ESKAPEE group of highly resistant and lethal pathogens where integrons are prevalent. We introduced all PICs into *K. pneumoniae* KP5, a MDR clinical isolate. We sequenced the genome of this strain and found three plasmids, one of which contains a class 1 integron (the full resistome can be found in Figure S5). The PHASTEST software did not detect prophages in the genome of KP5. We subjected all strains to infection with the *Drexlerviridae* phage F13 co-isolated with the strain. All PICs, except *picN*, demonstrated resistance to F13 at low MOI. Most of them also conferred resistance at high MOI (except *pic76*, *pic113*, *pic217*, and *picWGS21*) (Figure 2C). To introduce PICs in *P. aeruginosa* PAO1 strain, we changed the p15A origin of replication of pMBA for BBR1, and introduced a tetracycline resistance marker. After several assays, we could only transform *picN* successfully, while other PICs produced no colonies at all or abnormal (sick) colony morphologies (Figure 2D). This led us to hypothesize that some *pics* might be toxic or extremely costly in this background. To avoid this, we changed the strong promoter guiding the

270 expression of cassettes in pMBA (PcS) for a weaker version (PcW). This way we could
271 introduce *pic24, pic113, pic142* and *picWGS21* in PAO1 and were able to measure their
272 activities. We confronted these strains to a collection of 36 phages infecting PAO1 using a
273 double spot screen. We observed growth for *picN*, *pic142* and *picWGS21* in presence of phages
274 Vs1, Px4 and Px5. We evaluated the level of resistance by monitoring growth curves for each
275 PIC against the three phages, and confirmed their resistance phenotype (Figure 2C). *pic142* -
276 that had a clear phenotype against several phages both in *E. coli* and *K. pneumoniae*- confirmed
277 its broad spectrum and host range, conferring resistance to Px5 at both MOI and to Px4 at low
278 MOI ; contrarily, *picN* and *picWGS21,* that had only showed low resistance against a handful
279 of phages in *E. coli*, conferred very high resistance against phage Px4 and Vs1 in *P. aeruginosa*.
280 Altogether, our data proves that PICs can confer resistance to different phages and in different
281 host species. Although some PICs seem to have a defined narrow host range, others, like *pic142*
282 were able to confer resistance in the three species against most phages tested, underlying the
283 broad-spectrum activity of this defense mechanism.
284
285 **PICs protect against prophage activation.**
286 An important aspect of the interplay between phages, their hosts, mobile genetic
287 elements and defense systems is the case of prophage activation. Hindering activation of
288 prophages can both protect at the cell and at the population level. Here we asked if a plasmid
289 carrying a mobile integron with a PIC can limit the production of phage particles from a
290 chromosomally encoded prophage once it switches to lytic cycle. To test this, we introduced all
291 PICs in lysogens of *E. coli* 594 with either HK544 or Φ80 prophages in their genomes. We
292 induced prophage activation with mitomycin and quantitated the phage titer after 6 hours.
293 *pic128*, *pic135* and *pic142* showed mild to strong defense against the activation of HK544, with
294 20 to 1.000 fold decreases in plaque forming units. Pic59 completely abolished the production
295 of HK544 virions, showing $>10^7$ fold protection (Figure 3A). Resistance against Φ80 activation
296 was generally low, with only *picN, pic167,* and *pic233* producing statistically significant
297 resistance levels. Interestingly, there is not a clear correlation between defense against the free
298 form of the phage (Figure 1C) and the activation of the prophage. Certain systems, like *pic135*
299 and *pic142* confer resistance against both forms of a phage (HK544); while others, like *pic128*,
300 *pic167*.2 and *pic217* only conferred resistance against one. These results show that mobile
301 integrons containing PICs can interfere with prophage activation, highlighting the potential
302 protective effect at the community level, and the complex interplay between mobile genetic
303 elements.

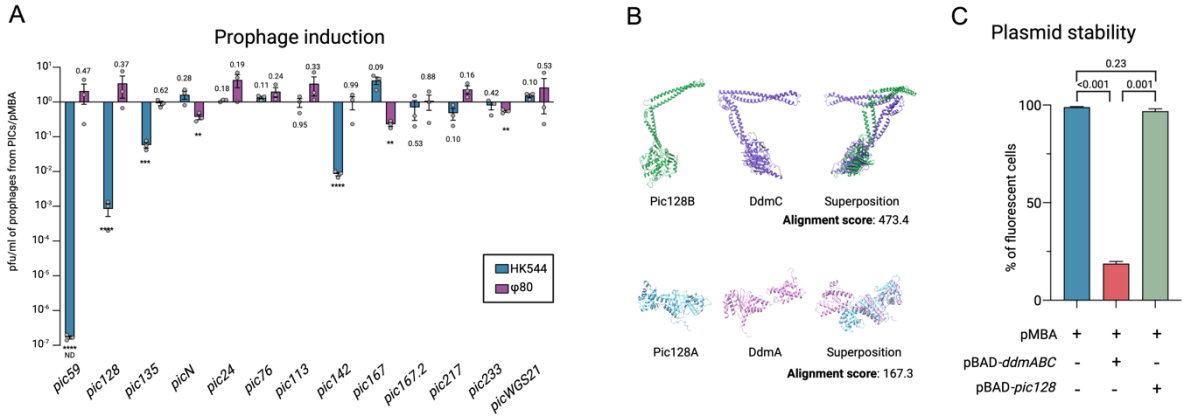

Figure 3. Prophage Induction, Structural Alignment, and Impact of *pic128* on Plasmid Stability. **(A)** Prophage induction assays inducing with mitomycin (0,5 µg/ml). The graph shows the concentration of phage (measured as plaque-forming units per millilitre (pfu/ml)) when activating prophages in the presence of pMBA containing PICs over the empty pMBA. ND: not detected (Limits of detection plotted). One sample *t* and Wilcoxon test; *P* values are shown when possible; ** < 0.01; *** < 0.001; ****<0.0001. **(B)** Structural alignment using FoldSeek of Pic128A and Pic128B proteins with known phage and plasmid defense proteins DdmA and DdmC, respectively. Superposition of protein structures is shown, with alignment scores indicating the degree of structural similarity. **(C)** Plasmid stability assays in *E. coli*. The percentage of fluorescent cells, representing the stability of pMBA, is shown for strains containing the pBAD plasmid with either the *ddmABC* or *pic128AB* systems. While *ddmABC* significantly reduces plasmid stability, *pic128* does not show a significant effect, indicating no anti-plasmid activity. Bars represent the mean of at least 3 biological replicates. Error bars correspond to the standard error of the mean. Statistical significance was assessed through unpaired t-tests and *P* values are shown.

pic128 does not have anti-plasmid activity.

DdmABC is a phage and plasmid defense system. It has been shown to confer phage resistance in *E. coli* and to cure plasmids in *Vibrio cholerae*, particularly those with a p15A replication origin[37]. When modelling protein structures of PICs, we found strong similarities between Pic128B and DdmC (Figure 3B), proteins that belong to (different) Lamassu defense systems. Interested by the interactions between mobile elements, we set out to examine whether the expression of *pic128AB* could exert a similar influence on plasmid stability. Because pMBA has a p15A replication origin, we decided to investigate the antiplasmid activity of *pic128AB* from a different vector. We hence cloned *pic128AB* and *ddmABC* systems into a pBAD plasmid that possess a pBR322 origin of replication and co-transformed them with an empty pMBA. We induced both systems with arabinose and monitored the loss of pMBA as the presence of non-fluorescent colonies for 3 days (ca. 20 generations). pMBA is stably maintained in the absence of antibiotics, with 99% of the cells in the population being fluorescent after 3 days. As expected, DdmABC strongly decreased the proportion of fluorescent colonies to 19% by day 3 (Figure 3C), while pMBA was stably maintained at >97% in the presence Pic128AB. This suggests that, despite their structural similarities, Pic128AB does not have the anti-plasmid activity detected for DdmABC. Still, both systems could have different plasmid specificities,

334 so we extended our plasmid stability studies to KP5, carrying the three distinct natural plasmids
335 conferring resistance to tetracycline, ertapenem and cefotaxime, respectively. After introducing
336 pMBA-*pic128* into this isolate we assessed plasmid stability monitoring the loss of three
337 resistance phenotypes conferred by these replicons over a five-day period (Figure S5). We could
338 not observe a significant plasmid loss in any case, suggesting that *pic128* is not an anti-plasmid
339 system.

340 **PICs entail different fitness effects that vary across species.**

341 A major question in the field of phage defense is how these systems affect the fitness of
342 the host. This has important implications in the accumulation of such systems in genomes and
343 in their spread between species. Integrons are known to be low-cost platforms that can modulate
344 the expression of the genes in their cargo by changing their position in the array[21,50,51]. Yet the
345 cost of each cassette can be different, which is of importance in their dispersal through HGT.
346 To determine the cost of PICs, we performed competition assays in both *E. coli* and *K.*
347 *pneumoniae* (Figure 4). In these experiments two strains that are isogenic -except for the PIC
348 and a fluorescent marker- are mixed and grown together. Using flow cytometry, the ratio of the
349 mixture is measured before and after growth, and changes in this ratio serve to quantitate the
350 cost of cassettes (see Materials and methods). Our results showed a broad distribution of fitness
351 effects among PICs, ranging from large costs (ca. 40%) to virtually costless in both species. In
352 *E. coli, pic217*, *pic128* and *picN* seemed to have a mildly positive impact in fitness (up to 3%)
353 suggesting that acquisition of certain systems can be costless (Figure 4A). It is of note, that here
354 we have used a strong version of the Pc promoter, which likely maximizes the cost of cassettes.
355 Weaker promoters are also found in MIs, so it is possible that the cost of cassettes is lower in
356 other integron platforms. Interestingly, fitness effects were not conserved between genetic
357 backgrounds. For instance, *picWGS21* entailed a small cost (ca. 7%) in *E. coli* but was very
358 costly (ca. 30%) in *K. pneumoniae* (Figure 4B). Only a few cassettes, like *picN* showed very
359 similar cost in both species. The lack of cost of PICs in certain genetic backgrounds, and the
360 differences in fitness effects across backgrounds can be of importance in the accumulation of
361 cassettes and their preferential distribution of PICs among species.

362 In the case of costly defense systems, a key advantage that integrons can provide to the
363 host, compared to encoding them elsewhere, is that they can modulate their expression. Cassette
364 expression dependes on its proximity to the Pc and on the polar effects that cassettes upstream
365 can exert. Because the expression of a gene and its fitness cost generally correlates, we
366 hypothesize that integrons can modulate the fitness of PICs in the array by modifying its
367 position in the array. To test this, we compared the cost entailed by *pic24* when located in first

368 position (see above) with the cost it entails when encoded in third position (as it is found in the
369 databases (Figure 2A)). For this, we constructed an array (pArrayØ) containing two antibiotic
370 resistance cassettes, with strong polar effects (*aacA54* and *aacA8*)[51], and introduced *pic24*
371 downstream, as a third cassette (pArray-*pic24*). Competition experiments show that while *pic24*
372 conferred a fitness cost of 11% when located in first position, it had no significant cost when in
373 third position (Figure 4C). This was indeed due to the strong repression of its expression, since
374 phage infection experiments showed pArray-*pic24* did not protect against T7 infection. Hence,
375 costly PICs can be carried by mobile integrons at no cost to be later reshuffled into first position,
376 providing phage resistance (*adaptation-) on demand*[24] We also show that PICs exert polar
377 effects on downstream cassettes (Figure 4D), participating in the modulation of function and
378 cost that we have previously demonstrated for antimicrobial resistance genes[51].
379

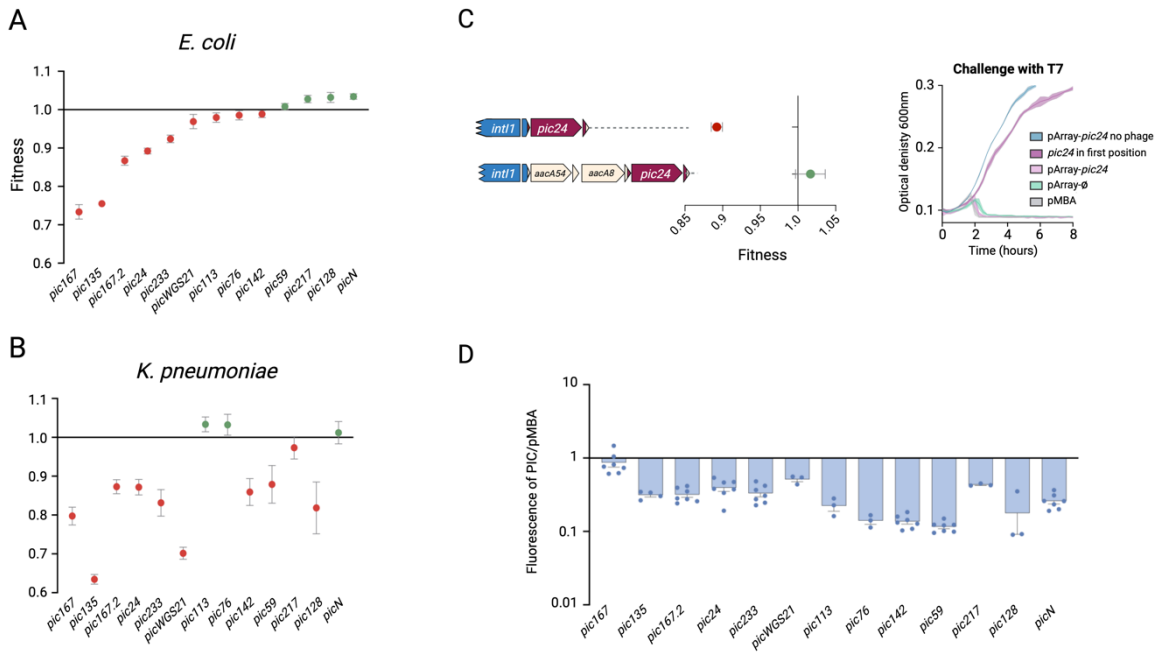

380
381 **Figure 4. Fitness Effects of PICs.** Fitness effects of PICs in **(A)** *E. coli* and **(B)** *K. pneumoniae*. Red circles represent fitness values below 1
382 (cost), while green circles indicate fitness values above 1 (gain). Fitness effects vary in sign and magnitude and are not conserved among
383 genetic backgrounds. **(C)** Modulation of fitness cost and function by integron position. The graph shows the fitness effect of *pic24* in first
384 position (competing pMBA vs pMBA-*pic24*) and third position (pArrayØ *vs.* pArray-*pic24*). The fitness cost imposed by the PIC is reduced
385 in third position behind cassettes with strong polar effects. The cost is related to the function of the PIC since pArray-*pic24* does not confer
386 resistance to T7. **(D)** Polar effects of PICs. All cassettes except *pic167* exert polar effects on downstream cassettes, limiting their expression.
387 All assays have been performed at least three times. Error bars represent the standard error of the mean.
388

389

390 **Mobile Integrons can accumulate resistance to phages and antibiotics.**

391 The fact that integrons carry defense systems is important in the ecology and biology of
392 these systems. Integron cassettes can be stockpiled, and their phenotypes can be additive, as we
393 have observed for multi-drug resistance MIs. It is hence possible that integrons can combine
394 PICs to provide multi-phage resistance; or PICs and antimicrobial resistance cassettes (ARCs)
395 providing phage- and AMR. This is important for phage therapy, since integrons would likely
396 play again -as it occurred with antibiotics- a key role in the evolution of resistance. Hence, we
397 sought to test if phage defense phenotypes can be additive and combined with antimicrobial
398 resistance genes. To do so, we first constructed pArray-1 an integron combining *pic24* ($T7^R$)
399 and bla_{OXA-10}, a class D β-lactamase gene that confers resistance to carbenicillin. The strain
400 carrying pArray-1 showed high levels of resistance against T7 and carbenicillin both separately
401 and simultaneously (Figure 5A). We then constructed pArray-2 containing *pic24* and *pic167.2*
402 (Figure 5A) that confer high and intermediate resistance to phage T7 and P1, respectively.
403 Strains carrying pArray-1 showed high resistance against both T7 and P1, highlighting the
404 additivity of phage resistance phenotypes. Our results show that, as predicted by the integron
405 model, integrons can combine phage resistance with AMR. Because MIs are enriched in AMR
406 genes, we can find several natural examples of the former among our PICs, with *picN*, *pic113*,
407 *pic167*, *pic217* and *picWGS21* located in integrons containing resistance genes against beta-
408 lactams, aminoglycosides, chloramphenicol and trimethoprim (Figure 2A). Because *gcus* are
409 less abundant, we did not find co-occurrence of PICs within an array. Nevertheless, having
410 described a variety of two-gene PICs, the genetic environment of *pic24* caught our attention
411 and was re-evaluated. This PIC is in a class 2 integron, preceded by two cassettes containing
412 two ORFs each. A new search with an updated version of DefenseFinder (June 2024) found
413 homologs of sensor protein ThsB from the Thoeris system in both cassettes (*gcu23* and *gcu24*).
414 It also found a type II restriction modification system downstream the last cassette of the
415 integron (Figure 5C). Both cassettes share 50% bp identity, and the ORFs share 17 and 37%
416 identity in amino acid sequence respectively. Nevertheless, the structure of the proteins in both
417 systems is remarkably conserved. Despite the homology of Pic22A and Pic23A with ThsB from
418 Thoeris, Pic22B and Pic23B are shorter than ThsA (approximately 300 *vs*. 500 aminoacids of
419 ThsA), show a very low protein identity (ca. 13%) and a very different predicted fold,
420 suggesting that these genes are not homologs. The structure of these proteins is instead similar
421 to that of the Deva system (*picWGS21*) (Figure 1E).

422 Both *gcu22* and *gcu23* were in our initial collection, but were not selected in our
423 screenings. In the case of *gcu22* we had not observed resistance in any case, while *gcu23* was
424 discarded because it yielded inconsistent results. We investigated this in more depth and
425 sequenced a variety of colonies from our *gcu23* stock. This revealed that the frequent
426 interruption of the cassette by the insertion of IS1, which explained the inconsistent results in
427 our screenings. We interpreted this as a sign of high fitness cost, so to test both cassettes we
428 cloned them in a modified pMBA under the control of a weak Pc promoter (PcW) (30-fold less
429 active than the PcS[52]) and tested them against the panel of phages in *E. coli* and *K. pneumoniae*.
430 *gcu22* conferred low levels of resistance exclusively against phage F13 in *K. pneumoniae*, while
431 *gcu23* had a broader defense profile, including very high resistance levels against G4, MS2, F1
432 and T4) (Figure 5D). We hence redefined both cassettes as PICs (*pic22* and *pic23*) and, given
433 the apparent hybrid genetic structure mentioned before, we consider this a novel system that we
434 have called Tragantía (a deity with the upper body of a woman and the lower body of a snake).
435 Finally, we sought to prove experimentally that this natural arrangement of cassettes acts as a
436 defense island. Given that only the phenotypes of *pic23* and *pic24* are distinguishable, we built
437 pArray-3 with *pic23* and *pic24* under the control of a PcW and challenged it against T4 and T7.
438 This array conferred multi-phage resistance (Figure 5E), confirming that mobile integrons
439 naturally act as mobile defense islands and that they are already circulating among clinical
440 isolates[53].

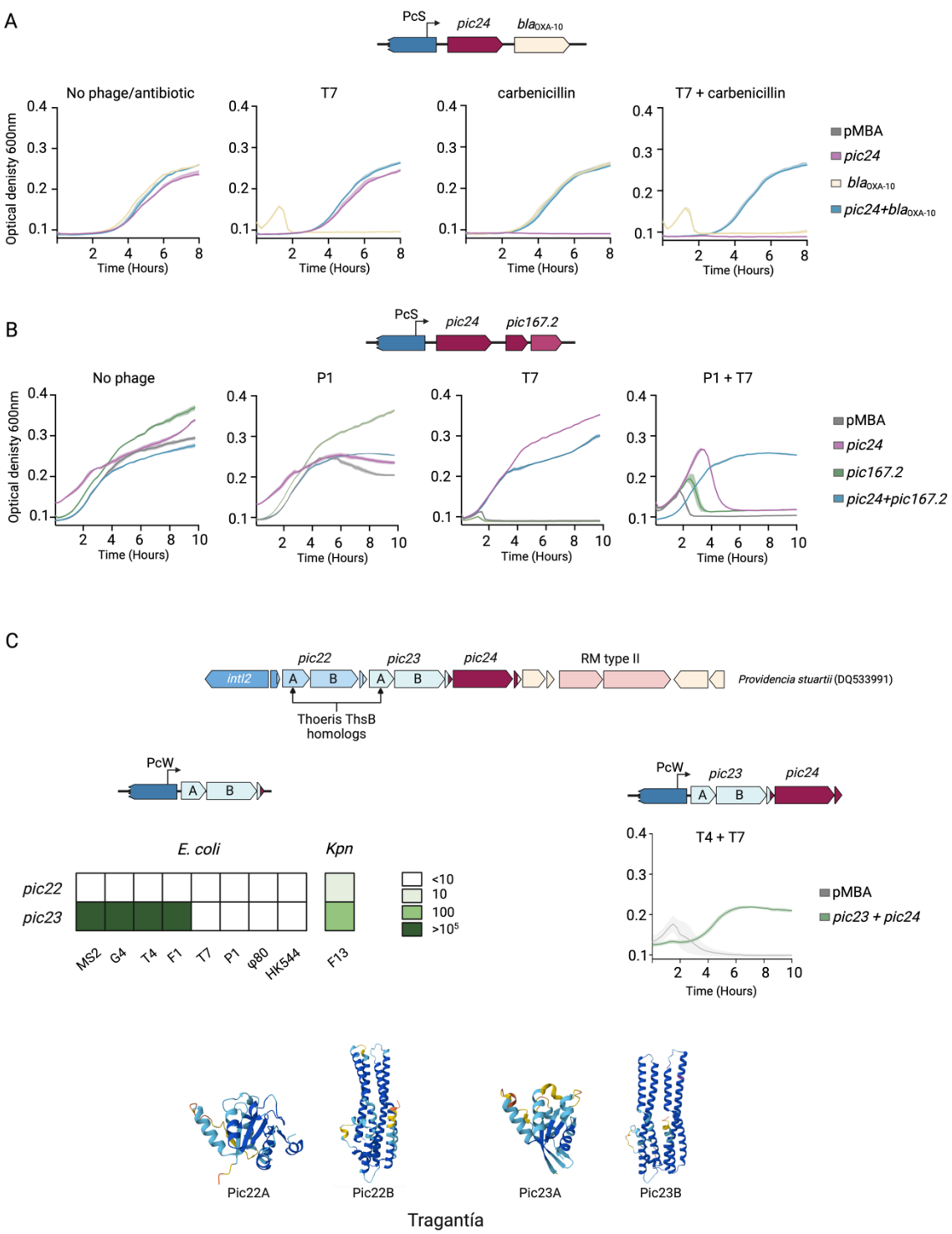

Figure 5. Additivity of Phage and Antibiotic Resistance Phenotypes in Multi-Cassette Arrays. Growth curves (OD_{600}) of *E. coli* strains containing **(A)** pMBA, *pic24* and *bla*$_{OXA-10}$ independently, and combined in an array in the absence of phage or antibiotic, and challenged with phage T7, carbenicillin, and a combination of both. The combined array confers resistance to phage and antibiotics simultaneously, and **(B)** pMBA, *pic24* and *pic167.2* independently, and combined in an array; either with no phage, or challenged with phage P1, phage T7, and a combination of both. (**C**) Genetic background of *pic24*. *pic22* and *pic23* contain homologs to TshB from Thoeris that confer resistance against phages from *E. coli* and *K. pneumoniae* (Kpn). *pic23* and *pic24* can confer multiphage resistance when in the same array. Growth curves are represented as the mean of three independent replicates. The standard error of the mean is represented as a lighter colour shade.

451 **Defense systems in PICs are found outside integrons.**

452 Integron cassettes are exchanged between integrons cohabiting the same cell. Mobile
453 integrons can therefore scan sedentary chromosomal integrons (SCIs) and bring to clinical
454 settings adaptive functions evolved elsewhere in the biosphere[54]. This suggests that PICs are
455 likely found in SCIs. In an article in this issue Darracq *et al*. provide evidence that the
456 Superintegron in *V. cholerae* contains indeed a variety of PICs, confirming their role as
457 biobanks of phage defense systems[55]. All the PICs in that work contain systems that are different
458 from the ones described here. We hence sought to investigate the potential origin and
459 distribution of our defense systems. We have searched for homologs in NCBI and examined the
460 genetic context of hits. Certain cassettes show a broad distribution among integrons (Figure
461 S6). Such is the case of *picN,* found among MIs and SCIs within the family *Pseudomonadaceae*
462 (Figure 6A)*,* which is consistent with it conferring resistance in *P. aeruginosa* (Figure 2C) and
463 exemplifies again how integrons connect clinical and environmental genomes. The defense
464 system Cosus was initially identified in *pic24* as part of a class 2 integron. Homologs of Cosus
465 are found as PICs in integron arrays in *Marinobacter salexigens* (Figure 6B). They are also
466 found in the genomes of *Vibrio* species, outside their SCIs but with a conserved *attC* site
467 suggesting that this could be a *bona fide* cassette integrated into an *attG* site in the chromosome
468 [56]. Interestingly, homologs of PicN and Pic24 were found isolated in the genomes of *Kangiella*
469 *japonica* and *Escherichia marmotae* without recognisable *attC* sites despite the sequence
470 conservation along the coding region (Figure 6C and Figure S7). Additionally, a Tragantía
471 system showing 95% aminoacid identity with Pic22A and B, is found in the chromosome of
472 *Marinobacter sp.* CuT6 (Figure 6D). This isolate has a complete integron and a cassette array
473 lacking an integrase (CALIN), but Tragantía is not in these regions. It is found within a small
474 defense island followed by homologs of Thoeris and Gao[57]. Yet compared to Pic22, this
475 Tragantía system has a pseudo *attC.* While canonical *attC* sites have two or three extrahelical
476 bases on one side of the stem -that act as landmarks for the integrase- and a conserved
477 GTT/AAC crossover point in the R box, this site has extrahelical bases at both sides of the stem,
478 and a mismatch in the conserved crossover point, which likely makes it non-recombinogenic
479 (Figure S8). While this does not seem to be a *bona fide* integron cassette (and it is not recognised
480 by IntegronFinder), it is strikingly close (only a few mutations away) from a canonical one.
481 Altogether, this highlights the high plasticity in the genetic context of the systems encoded in
482 PICs and suggest a recent recruitment of these systems into integrons.

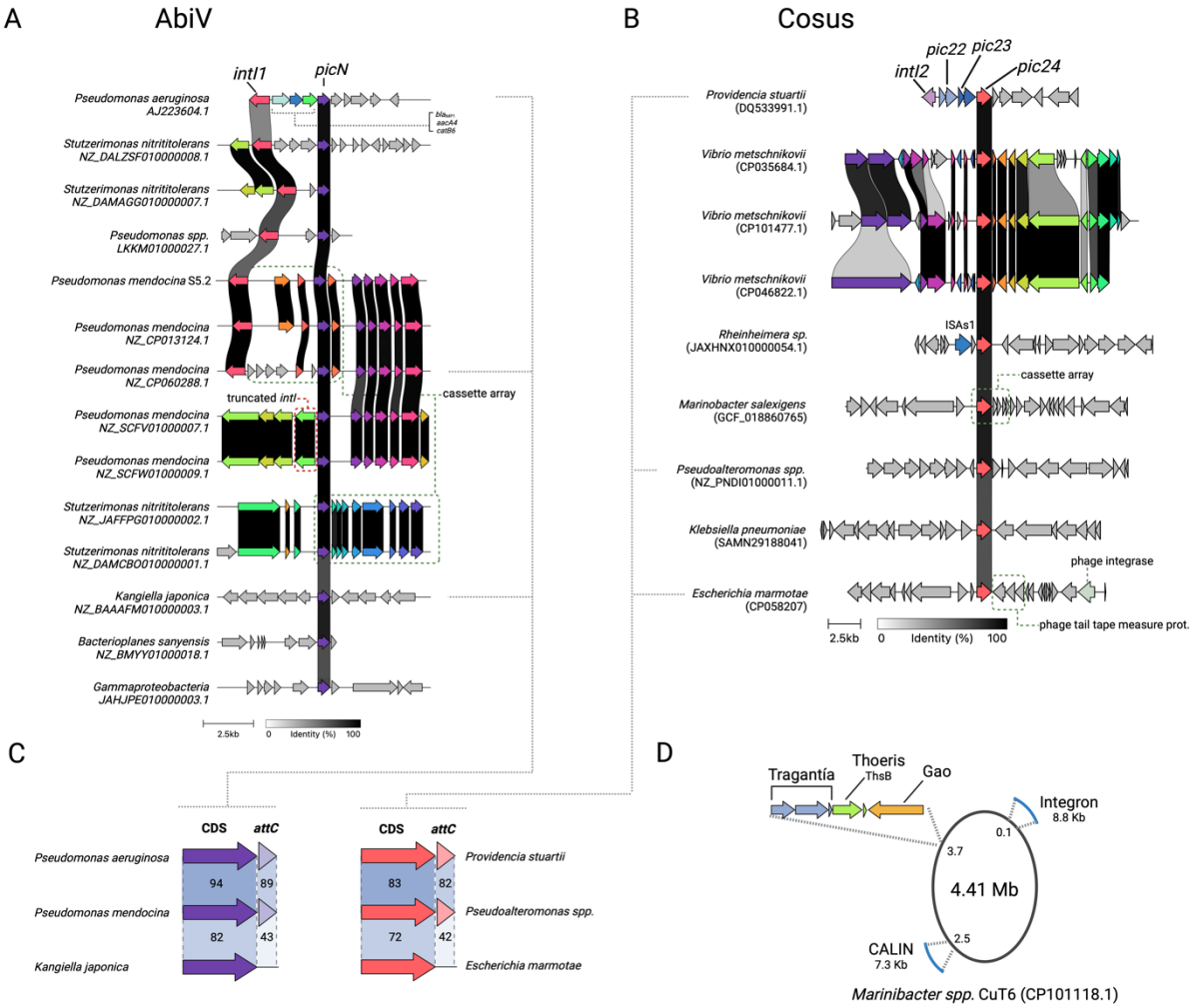

Figure 6. Genetic context of PIC homologs. Analysis of the genetic environments of AbiV (*picN*) **(A)** and Cosus (*pic24*) **(B)** showing their distribution in mobile and sedentary chromosomal integrons of different species. Integron integrases and arrays are marked where recognised. Some homologs to PICs are also found in outside integrons, and, despite a good sequence conservation in the coding region, they lack *attC* sites (**C**). A Tragantia system, homolog of *pic22,* is found within a small defense island in the chromosome of *Marinibacter* spp. and contains a pseudo *attC* site. This isolate contains an SCI and a CALIN.

490 **DISCUSSION**

491 Phage therapy is an old approach with renewed interest in the light of the AMR
492 crisis[58,59]. It allows for personalized treatments against multidrug resistant bacteria, with
493 encouraging outcomes. Phage resistance is a rapidly evolving field of research. The constant
494 discovery of new resistance genes, often encoded in defense islands and prophages, reveals the
495 intense arms race between bacteria and their phages, and between mobile genetic elements. We
496 lack knowledge on how defense systems are recruited into these islands and on how frequently
497 they can move through HGT[13]. In contrast, mobile integrons are highly adaptable genetic
498 elements that have significantly contributed to the proliferation of multidrug resistance bringing
499 to our hospitals a plethora of resistance cassettes from the genomes of environmental bacteria.
500 Being shed to the environment at extremely high quantities (10^{23} per day)[60], mobile integrons
501 have established a strong communication route between the genomes of pathogenic and
502 environmental bacteria[61]. Hence, the rampant movement of mobile integrons among clinically
503 relevant bacteria ensures a high speed of dissemination of novel adaptive functions throughout
504 our hospitals. It is therefore critical for the future of phage therapy to understand the potential
505 role of integrons in phage defense. In this work we confirm that mobile integrons already
506 contain such systems.

507 We have successfully identified 15 PICs using bioinformatic tools and a phenotypic
508 screening. As is the case of most defense systems, PICs displayed different specificities
509 conferring narrow to broad immunity in our assays. Nevertheless, because integrons can build
510 arrays of cassettes, they can combine phenotypes to confer multi-phage or phage-drug
511 resistance, the same way they currently confer multidrug resistance. In fact, *picN* is already
512 found in an array with at least three ARCs in a *P. aeruginosa* clinical isolate (Figure 2A). This,
513 and other examples of integrons containing PICs at different positions within the array, together
514 with our results showing that they can be carried at no cost, suggest that mobile integrons can
515 become low-cost, highly-mobile defense islands. An extreme case of this is shown by Darracq
516 *et al*. in a back-to-back paper in this issue, where they describe the presence of PICs in the
517 Superintegron of *Vibrio cholerae*. Indeed, in a recent work we have shown that the
518 Superintegron is carried at no measurable cost [62]. Additionally, their findings proves that
519 chromosomal integrons are virtually infinite repositories of PICs from where they can be
520 recollected by mobile integrons. Both Darracq *et al*. and us show that *pics* are functional in
521 distant genetic backgrounds. In our work, we show that this is the case in 3 of the 5 Gram
522 negative species and strains of the ESKAPEE group of highly resistant and dangerous
523 pathogens: the kind of bacteria aimed by phage therapy assays. This strongly suggests that the

524 spread of PICs among them will be quick if selective pressure with phages becomes
525 commonplace. This has implications in what are today considered as exploitable trade-offs in
526 phage therapy. For instance, it is known that many *K. pneumoniae* phages bind the bacterial
527 capsule and that resistant clones can easily arise through capsule loss, albeit at the cost of
528 becoming non-virulent[63]. Also, in some cases becoming resistant to phage infection through
529 mutations comes at the cost of losing antibiotic resistance[64,65]. The acquisition of plasmids
530 containing integrons with PICs can abrogate the exploitability of such trade-offs, rendering
531 virulence and antibiotic resistance perfectly compatible with phage resistance.

532 The role of mobile integrons in phage resistance exemplifies the interplay between
533 mobile genetic elements. Indeed, many of the PICs described here confer resistance against
534 phages that target the conjugative pilus of *E. coli* IJ1862. Hence, PICs can be beneficial for
535 conjugative plasmids that protect indirectly protecting their host. This way Mobile Integrons
536 would alleviate the trade-off between acquiring adaptive in plasmids and becoming susceptible
537 to a large variety of phages. Another aspect of this complex interplay is the potential link of
538 *pic128* with plasmid stability. Contrarily to the *ddmABC* system, *pic128* does not interact with
539 p15A plasmid or with any natural plasmids present in KP5. This result highlights that not all
540 Lamassu systems have the same activity toward plasmids. The lack of anti-plasmid activity in
541 Pic128AB might have a biological meaning. Given that plasmid acquisition is an important
542 source of antibiotic resistance, it is possible that the lack of anti-plasmid activity of *pic128* has
543 been selected for in an environment with high antibiotic pressure. Additionally, the fact that
544 certain pics could not be introduced in *P. aeruginosa* (even under a weak Pc promoter) suggests
545 that PICs can act as barriers to HGT.

546 Our work is not exempt of limitations. First, our screening -while successful in detecting
547 nine new genes- was based in the use of only T4 and T7. Given that some *pics* exhibit high
548 specificity against phages, it is likely that the number of *pic*s present in our collection of *gcus*
549 is underestimated. This could also apply to prophage-activation protection and plasmid stability
550 assays, if additional prophages and plasmids were tested. Additionally, algorithms to detect
551 defense systems are being constantly improved, so that detection of PICs in *gcus* will likely be
552 more prolific at the time this work is published.

553 This study shapes our perception of integrons. The presence of phage defense systems
554 and antibiotic resistance genes, proposes that integrons are protection elements against a large
555 breadth of environmental insults. This can guide the search for novel functions in the virtually
556 infinite reservoir of cassettes in nature. Our data also suggest that defense systems have been
557 recruited recently in integrons, providing for the first time, a multitude of examples of closely

558 related homologs of cassettes that are not part of integrons. We have also found an example of
559 a Tragantía system with a pseudo *attC* sites that is only a few mutations away of becoming a
560 fully recombinogenic *attC*. This way, the study of PICs can help understand how genes become
561 cassettes, a long-standing question in the field. Our results have also important implications in
562 the field of phage resistance, where mobile integrons provide extreme mobility at a very low
563 and adjustable fitness cost. Finding defense systems in Mobile integrons highlights the risk that
564 phage resistance genes could follow the same dissemination route as ARG in the past century.
565 The field of phage therapy must be vigilant about the adaptive power of integrons: selective
566 pressure will most likely reveal once again a major role of integrons in the spread of resistance
567 mechanisms. If the importance of integrons in the evolution of phage resistance is neglected, it
568 might come a day when phage hunting against clinical isolates becomes extremely difficult.
569

570 **MATERIAL AND METHODS**

571 **Strains and Phage collection**

572 A list of strains can be found in Table S1. *E. coli* DH5a and *P. aeruginosa* PAO1 are laboratory
573 strains. *K. pneumoniae* KP5 is a clinical isolated at Hospital Fundación Jiménez Diaz, Madrid.
574 *E. coli* 594[66], was kindly donated by José Penadés together with phages HK544 and Φ80.
575 Strains were grown at 37 °C in lysogeny broth (LB) or LB agar (1.5 %) (BD, France). Zeocin
576 was added at 100 µg/ml to maintain pMBA and pMBA-derived plasmids in *E. coli* and *K.*
577 *pneumoniae*. Tetracycline at 100 µg/ml was used to maintain pMBA plasmids in *P. aeruginosa*.
578 Liquid cultures were incubated in an Infors Multitron shaker at 200 rpm (Informs HT,
579 Swiss). Antibiotics were purchased from Sigma Aldrich (Merck, USA) except for zeocin
580 (InvivoGen, USA).

581 The coliphages included T4, T7, P1, MS2, G4, F1 which belong to the *Myoviridae*,
582 *Autographiviridae*, *Myoviridae*, *Fiersviridae*, *Microviridae* and *Inoviridae*, respectively. *E. coli*
583 phage MS2, F1, G4 and their host *E. coli* IJ1862[42] were kindly provided by from Prof. James J.
584 Bull (University of Texas). Phages T4, T7, and P1 were purchased from the DMSZ collection
585 (Leibniz, Germany). The *K. pneumoniae* phage, named F13, (found in effluents from a hospital)
586 was selected for its ability to lyse a clinical isolate called KP5, which produces the class D
587 carbapenemase OXA-48 and used as its host for this study. We computed the genomic data
588 obtained by Illumina technology with PHASTER to determined that F13 belongs to the
589 *Drexlerviridae* family. The *P. aeruginosa* PAO1 strain was used as a host for the Px4, Px5 and
590 Vs1 phages used in this study.

591 **Phage production**

592 We prepared phage solutions using previously published protocols[67]. Briefly, we grew host
593 bacteria in LB broth at 37ºC until they reached the exponential phase. At that point, we initiated
594 and monitored infection with the respective phage for 4 (for T7, T4, P1 phages) to 6 hours (for
595 MS2, G4, F1, HK544, and Φ80 phages). When we observed a decrease in optical density (OD),
596 we allowed the lysis process to continue for an additional hour. We then transferred the cultures
597 to polystyrene Falcon tubes for centrifugation and subsequent filtration using a 0.2 µm filter
598 (Sartorius, Spain) to collect the lysate containing the phage. Next, we titered the phage solutions
599 to determine the plaque-forming units (PFU). For plating, we mixed bacterial cultures (OD_{600}
600 ~1) with top agar medium and poured it onto agar dishes. After allowing it to dry for 30 minutes,
601 we spotted serial dilutions of the phages onto the agar plates and incubated them overnight at
602 37ºC[68].

603 ***In silico* analysis**

604 We generated the list of *gcus* using the INTEGRALL database (integrall.bio.ua.pt) and Integron
605 finder[33,44]. To determine if the *gcus* associated with known phage resistance defense systems,
606 we subjected the sequences of all *gcus* to a BLAST search against the two main defense system
607 databases: DefenseFinder[69] and PADLOC[35]. For *gcus* that showed a resistance phenotype but
608 remained unidentified by these platforms, we used an AlphaFold2 pipeline known as ColabFold
609 for prediction, followed by Foldseek to gain insights into the protein function of each *gcu*[70,71].
610 Additionally, we employed the Iterative Threading ASSEmbly Refinement (ITASSER)
611 platform to leverage complementary approaches for protein function prediction[72]. Genetic
612 environments were anlayzed with CAGECAT (cagecat.bioinformatics.nl)[73].

613 We carried out the sequencing of the *K. pneumoniae* isolate KP5 using a combination of
614 Illumina and Nanopore technologies, with SeqCoast (Portsmouth, USA) performing the
615 sequencing. We performed genome assembly using Unicycler software and conducted
616 subsequent analyses using the Center for Genomic Epidemiology platform. We determined the
617 resistome using the ResFinder web platform, identified the sequence type using MLST, and
618 characterized the plasmids using the PlasmidFinder web platform[74–76]. We assessed the
619 presence of prophages in the genome using the PHASTER web tool[77]. General DNA sequence
620 analysis was performed with Geneious and figures were created with BioRender.com.

621 **Cloning *gcu*s in pMBA**

622 All *gcus* were synthesized as double-stranded DNA by IDT ((Newark, USA), with an addition
623 of a 20 bp homology region corresponding to the targeted cloning site of pMBA located between
624 the *intI1* and *gfp* gene[32]. We performed the cloning process using the Gibson assembly method[78]
625 and selected clones on an LB agar plate supplemented with zeocin (50µg/mL). We cloned the
626 entire sequences of the *gcus*, including the open reading frame (ORF) and their *attC* region,
627 into the pMBA vector. Our in-house designed pMBA plasmid contains a p15A replication
628 origin, a zeocin resistance marker, and a truncated *intI1* gene followed by a *gfp* gene, acting as
629 a second integron cassette. We inserted the cloned *gcus* as the first cassette in the vector. To
630 ensure a relevant level of expression for each *gcu*, we selected a strong version of the Pc
631 promoter, PcS, located within the *intI1* gene, for our constructions. For the construction of
632 pArray-1 and pArray-2, we cloned at second position of the integron-like structure of pMBA
633 the $bla_{\text{OXA-10}}$ gene or the *pic167.2* instead of having the *gfp* gene, respectively. For the
634 construction of pArray-3, we cloned *pic23* and *pic 24* at first and second position, respectively,
635 of the integron-like structure present in pMBA under the control of a PcW promoter.

636 The construction of pArrayØ was accomplished using the Gibson assembly protocol, wherein
637 the *aacA54* and *aacA8* resistance gene cassettes were cloned into the pMBA-Δ*gfp* vector.
638 Subsequently, pArray-*pic24* was created by cloning the *pic24* gene into the third position of the
639 synthetic integron, downstream of the *aacA8* gene cassette.
640 For the cloning of *gcus* into *Pseudomonas aeruginosa* PAO1, we used a modified pMBA vector
641 (pBTZ). The p15A replication origin was replaced with the BBR1 origin to ensure replication
642 in both *E. coli* and *P. aeruginosa* species. Additionally, the strong PcS promoter was substituted
643 with its weaker version, PcW. Finally, a tetracycline resistance marker was introduced, as
644 *P. aeruginosa* exhibits low resistance to zeocin. The list of oligonucleotides used can be found
645 in Table S2. The sequences of PICs can be found in Table S3.
646 **Growth curves and phage lysis monitoring**
647 We inoculated a single colony of a clone carrying a potential phage resistance gene into an
648 overnight culture of Luria Bertani (LB) broth at 37ºC. The next day, we adjusted the culture to
649 an optical density of 0.1 and transferred it to a 96-well plate containing LB broth supplemented
650 with zeocin (50 µg/mL). We then exposed the plate to different concentrations of phage to test
651 various multiplicities of infection (MOI). For all tested phages, we defined a high MOI
652 condition as an MOI of 1 and a low MOI condition as an MOI of 0,01. However, for phages T4
653 and T7, which exhibit high lytic activity, we set the high MOI condition to 0,01 and the low
654 MOI condition to 0,00001. We monitored growth curves using a Biotek HTX synergy plate
655 reader (Agilent , USA) at 600 nm over a 16-hour period. To assess the phage lysis level, we
656 calculated the area under the curve (AUC) for each growth condition, both with and without
657 phage as described previously[43]. The inhibition score for each sample was calculated using the
658 following formula:

659 $$Inhibition\ Score = \left(\frac{\Delta AUC}{\Delta AUC_{no\ phage}}\right) \times 100$$

660 where ΔAUC is the difference in AUC between the conditions with and without phage.
661 Specifically, $\Delta\mathrm{AUC} = \mathrm{AUC}_{no\ phage} - \mathrm{AUC}_{phage}$. We calculated the inhibition scores for both
662 high and low multiplicity of infection (MOI) conditions. These scores were then normalized by
663 comparing them to the inhibition scores obtained from the control samples, which used the
664 empty pMBA vector. The normalization was done by computing the ratio of the inhibition score
665 of the experimental sample to the inhibition score of the control: $Inhibition =$
666 $\left(\frac{Inhibition\ Score_{pic}}{Inhibition\ Score_{pMBA}}\right) \times 100$. By using the "inhibition score", we normalize the reduction of the
667 area under the curve relative to growth without the phage. This allows for comparison of the

668 relative effects regardless of initial growth differences between strains. The protective effect of
669 the PIC is shown as the inverse of the inhibition score.

670 **Prophage activation assay**

671 We chemically activate the lytic cycle of the prophages HK544 and Φ80 in E. coli 594::pMBA-
672 *pic* using mitomycin C at a concentration of 0,5 µg/mL. Briefly, we adjusted the culture to an
673 optical density of 0.1, and after 1h we induced prophage activation by adding mitomycin C.
674 Then, we quantitated the production of active phages after 6 hours of induction. To do so, we
675 centrifuged the culture we performed serial dilutions of the supernatant and spotted it on top
676 agar plate containing IJ-pMBA to evaluate the phage concentration[79].

677 **Phage-resistant clone screening**

678 To identify new phage defense integron cassettes, we employed both liquid and solid media
679 screening strategies. Initially, we cultured clones carrying various *gcus* overnight in LB broth
680 with zeocin (50 µg/mL). The following day, a 1 OD dilution of each culture (10 µL) was spotted
681 onto LB agar plates supplemented with zeocin. After 1 hour of incubation, we applied 7 µL of
682 phage T4 solution at a concentration of 10^9 PFU/mL to the bacterial spots. After 16-18 hours of
683 incubation, we selected the clones that exhibited growth despite phage presence for further
684 analysis. Additionally, we conducted a high-throughput screening in 96-well plates, challenging
685 the entire *gcu* collection with phages T7 and T4 under two different multiplicities of infection
686 (MOI) conditions, following the protocol described previously.

687 **Plasmid stability experiment**

688 We co-transformed *E. coli* IJ862 with both the empty pMBA plasmid carrying the p15A replicon
689 and the L-arabinose inducible pBAD plasmid carrying either the *pic128* or *ddmABC* defense
690 system. For five days, three replicates were put in culture in LB broth supplemented with
691 carbenicillin (100 µg/ml) and L-arabinose (0,1%). Daily, we transferred 50 µl of each culture
692 into fresh 5 ml LB broth and used another 50 µl to count GFP-expressing colonies on LB agar
693 plates supplemented with carbenicillin.

694 To assess the stability of the endogenous clinical plasmids in KP5 *K. pneumoniae* isolate, we
695 cultivated clones harbouring *pic128* in LB broth with zeocin (50 µg/ml) over five days. On days
696 1 and 5, we selected >120 colonies from LB zeocin agar plates and subcultured them onto
697 separate LB media containing either tetracycline (15 µg/ml), cefotaxime (50 µg/ml), or
698 ertapenem (30 µg/ml). This step aimed to detect any loss of resistance, which would suggest
699 the corresponding loss of one of the three natural plasmids.

700 ***attC* recombination experiments**

701 Recombination experiments were conducted as previously described[80]. Briefly, we cloned the
702 3' region of each *pic* using a pSW23T mobilizable plasmid containing a chloramphenicol
703 resistance marker into *E. coli* β2163 strain (*dapA*$^-$, *pir*$^+$) requiring diaminopimelic acid (DAP)
704 to grow. We used *E. coli* β2163 as donor strain for conjugation experiments using *E. coli* DH5α
705 strain carrying both a p3938 plasmid (Carb^R) containing an L-arabinose inducible *intI1* gene
706 and a p929 plasmid (Kana^R) containing an *attI* site as recipient. We performed conjugation
707 experiments onto LB agar supplemented with DAP and L-arabinose (0,2%) overnight. The next
708 day, after cell recover, we performed ten-folded dilutions onto LB agar supplemented with
709 carbenicillin (100 µg/ml) and glucose (1%) or with carbenicillin, glucose and chloramphenicol
710 (25 µg/ml) to select for the total population and recombinants, respectively.

711

712 **Fitness experiment**

713 To assess the fitness cost of each PIC, we performed *in vitro* competition assays following the
714 protocol described in[81] with some modifications. Briefly, we subcloned the panel of the 13 *PICs*
715 into a modified version of the pMBA vector, which includes a knock-out *gfp* gene (with a stop
716 codon instead of the start codon), along with an empty vector control. We then subjected this
717 new set of clones to a fitness competition experiment against the wild type pMBA vector
718 carrying the intact *gfp* gene. Briefly, we grew six replicates of each clone overnight at 37ºC in
719 a 96-well plate filled with LB broth supplemented with zeocin (50 µg/ml). The next day, we
720 mixed cells containing the target *gcu* in the pMBA-Δ*gfp* in a 1:1 volume ratio with the clone
721 carrying the pMBA-WT vector. We diluted these mixtures 1:20 in 96-well plates containing
722 NaCl 0,9%. This plate was further diluted 1:20 in a plate with NaCl and another with LB broth
723 supplemented with zeocin. The first plate was used to estimate the percentage of pMBA-WT
724 and pMBA-*pic*-Δ*gfp* cells in the mixture on day 1, using a Cytoflex S cytometer (Beckman
725 Coulter, USA). The second plate (with LB) was incubated overnight. The next day these
726 cultures were diluted 1:400 in NaCl to determine the proportion of strains in the mixture as
727 explained above. Following the formula described in[81], fitness cost was calculated as the
728 difference in ratios of GFP-fluorescence between day 1 and day 2 for each *PIC*.

729

730 **Quantitation of polar effects**

731 To determine the polar effects of cassettes, we measured the fluorescence of the Green
732 Fluorescent Protein (GFP) that acts as a second cassette in pMBA. At least three independent
733 colonies of each pMBA derived strain were inoculated in LB zeocin and incubated at 37ºC

overnight. Cultures were then diluted 1/400 in filtered saline solution to measure fluorescence using a Cytoflex-S flow cytometer (Beckman Coulter). The 488 nm laser was used to detect GFP expression through 525/40 nm (FITC) band pass filter. 20,000 events were recorded per sample. Data were analysed using CytExpert software (v.2.4; Beckman Coulter).

DATA AVAILABILTY:

The genome of strain KP5 has been deposited in NCBI GenBank (accession numbers: CP162381-CP162384)

CONFLICT OF INTERESTS

None to declare.

ACKNOWLEDGEMENTS

We would like to thank Dr. José R. Penadés and Dr. James J. Bull for providing phages and strains, and Tamara Barcos for technical assistance. We thank André Carvalho for critical reading of the manuscript. NK is supported by funding from the European Union's Horizon 2020 research and innovation programme under the Marie Skłodowska-Curie grant agreement No 847635 for the ANARC research project (No 4230415). The work in the MBA laboratory is supported by the European Research Council (ERC) through a Starting Grant [803375]; Ministerio de Ciencia, Innovación y Universidades [BIO2017-85056-P; CNS2022-135857]; Ministerio de Ciencia e Innovación [PID2020-117499RB-100] and the EU HARISSA JPI-AMR program [PCI2021-122024-2A]; A.H. is supported by the PhD program at UCM. PB is supported by the Juan de la Cierva program (FJC 2020-043017-I). P.D-C. was supported by a Ramón y Cajal contract RYC2019-028015-I and the project PID2020-112835RA-I00, funded by MCIN/AEI/10.13039/501100011033, ESF Invest in your future; MG-Q is supported by the Subprograma Miguel Servet from the Ministerio de Ciencia e Innovación of Spain (CP19/00104), Instituto de Salud Carlos III (Plan Estatal de I+D+i 2017–2020), and co-funded by European Social Fund "Investing in your future". J.A.E. is supported by the Atracción de Talento Program of the Comunidad de Madrid [2016-T1/BIO-1105, 2020-5A/BIO-19726];

764 **REFERENCES**

765

766 1. Antimicrobial Resistance Collaborators. Global burden of bacterial antimicrobial
767 resistance in 2019: a systematic analysis. *Lancet* **399**, 629–655 (2022).
768 2. d'Herelle, F. Bacteriophage as a Treatment in Acute Medical and Surgical Infections.
769 *Bull N Y Acad Med* **7**, 329–48 (1931).
770 3. Hatfull, G. F., Dedrick, R. M. & Schooley, R. T. Phage Therapy for Antibiotic-Resistant
771 Bacterial Infections. *Annu Rev Med* **73**, 197–211 (2022).
772 4. Kortright, K. E., Chan, B. K., Koff, J. L. & Turner, P. E. Phage Therapy: A Renewed
773 Approach to Combat Antibiotic-Resistant Bacteria. *Cell Host Microbe* **25**, 219–232
774 (2019).
775 5. Labrie, S. J., Samson, J. E. & Moineau, S. Bacteriophage resistance mechanisms. *Nat*
776 *Rev Microbiol* **8**, 317–27 (2010).
777 6. Rostøl, J. T. & Marraffini, L. (Ph)ighting Phages: How Bacteria Resist Their Parasites.
778 *Cell Host Microbe* **25**, 184–194 (2019).
779 7. Bernheim, A. & Sorek, R. The pan-immune system of bacteria: antiviral defence as a
780 community resource. *Nat Rev Microbiol* **18**, 113–119 (2020).
781 8. Labrie, S. J., Samson, J. E. & Moineau, S. Bacteriophage resistance mechanisms. *Nat*
782 *Rev Microbiol* **8**, 317–27 (2010).
783 9. Millman, A. *et al.* An expanded arsenal of immune systems that protect bacteria from
784 phages. *Cell Host Microbe* **30**, 1556-1569.e5 (2022).
785 10. Vassallo, C. N., Doering, C. R., Littlehale, M. L., Teodoro, G. I. C. & Laub, M. T. A
786 functional selection reveals previously undetected anti-phage defence systems in the E.
787 coli pangenome. *Nat Microbiol* **7**, 1568–1579 (2022).
788 11. Dedrick, R. M. *et al.* Prophage-mediated defence against viral attack and viral counter-
789 defence. *Nat Microbiol* **2**, 16251 (2017).
790 12. Hochhauser, D., Millman, A. & Sorek, R. The defense island repertoire of the
791 Escherichia coli pan-genome. *PLoS Genet* **19**, e1010694 (2023).
792 13. Makarova, K. S., Wolf, Y. I., Snir, S. & Koonin, E. V. Defense Islands in Bacterial and
793 Archaeal Genomes and Prediction of Novel Defense Systems. *J Bacteriol* **193**, 6039–
794 6056 (2011).
795 14. Ghaly, T. M. *et al.* The Natural History of Integrons. *Microorganisms* **9**, (2021).
796 15. Labbate, M., Case, R. J. & Stokes, H. W. The Integron/Gene Cassette System: An
797 Active Player in Bacterial Adaptation. in 103–125 (2009). doi:10.1007/978-1-60327-
798 853-9_6.
799 16. Mazel, D. Integrons: Agents of bacterial evolution. *Nat Rev Microbiol* **4**, 608–620
800 (2006).
801 17. Recchia, G. D. & Hall, R. M. Gene cassettes: A new class of mobile element.
802 *Microbiology (N Y)* **141**, 3015–3027 (1995).
803 18. Partridge, S. R. *et al.* Definition of the attI1 site of class 1 integrons. *Microbiology (N*
804 *Y)* **146**, 2855–2864 (2000).
805 19. Collis, C. M. & Hall, R. M. Expression of antibiotic resistance genes in the integrated
806 cassettes of integrons. *Antimicrob Agents Chemother* **39**, 155–162 (1995).
807 20. Barraud, O. & Ploy, M. C. Diversity of class 1 integron gene cassette rearrangements
808 selected under antibiotic pressure. *J Bacteriol* **197**, 2171–2178 (2015).

21. Souque, C., Escudero, J. A. & Maclean, R. C. Integron activity accelerates the evolution of antibiotic resistance. *Elife* **10**, 1–47 (2021).
22. Carvalho, A. *et al.* The expression of integron arrays is shaped by the translation rate of cassettes. doi:10.1101/2024.03.26.586746.
23. Guerin, É. *et al.* The SOS Response Controls Integron Recombination. *Science (1979)* **324**, 1034–1034 (2009).
24. Escudero, J. A., Loot, C., Nivina, A. & Mazel, D. The Integron: Adaptation On Demand. *Mobile DNA III* 139–161 (2015) doi:10.1128/9781555819217.ch6.
25. Partridge, S. R., Kwong, S. M., Firth, N. & Jensen, S. O. Mobile Genetic Elements Associated with Antimicrobial Resistance. *Clin Microbiol Rev* **31**, (2018).
26. Stokes, H. W. & Hall, R. M. A novel family of potentially mobile DNA elements encoding site-specific gene-integration functions: integrons. *Mol Microbiol* **3**, 1669–1683 (1989).
27. Domingues, S., da Silva, G. J. & Nielsen, K. M. Integrons: Vehicles and pathways for horizontal dissemination in bacteria. *Mob Genet Elements* **2**, 211–223 (2012).
28. Mitsuhashi, S., Harada, K., Hashimoto, H. & Egawa, R. On the drug-resistance of enteric bacteria. 4. Drug-resistance of Shigella prevalent in Japan. *Jpn J Exp Med* **31**, 47–52 (1961).
29. Kaushik, M., Kumar, S., Kapoor, R. K., Virdi, J. S. & Gulati, P. Integrons in Enterobacteriaceae : diversity, distribution and epidemiology. *Int J Antimicrob Agents* **51**, 167–176 (2018).
30. Hipólito, A., García-Pastor, L., Vergara, E., Jové, T. & Escudero, J. A. Profile and resistance levels of 136 integron resistance genes. *npj Antimicrobials and Resistance* **1**, 13 (2023).
31. Partridge, S. R., Tsafnat, G., Coiera, E. & Iredell, J. R. Gene cassettes and cassette arrays in mobile resistance integrons. *FEMS Microbiol Rev* **33**, 757–784 (2009).
32. Hipólito, A. *et al.* The expression of aminoglycoside resistance genes in integron cassettes is not controlled by riboswitches. *Nucleic Acids Res* (2022) doi:10.1093/nar/gkac662.
33. Moura, A. *et al.* INTEGRALL: A database and search engine for integrons, integrases and gene cassettes. *Bioinformatics* **25**, 1096–1098 (2009).
34. Tesson, F. *et al.* Systematic and quantitative view of the antiviral arsenal of prokaryotes. *Nat Commun* **13**, 2561 (2022).
35. Payne, L. J. *et al.* PADLOC: a web server for the identification of antiviral defence systems in microbial genomes. *Nucleic Acids Res* **50**, W541–W550 (2022).
36. Rousset, F. *et al.* Phages and their satellites encode hotspots of antiviral systems. *Cell Host Microbe* **30**, 740-753.e5 (2022).
37. Jaskólska, M., Adams, D. W. & Blokesch, M. Two defence systems eliminate plasmids from seventh pandemic Vibrio cholerae. *Nature* **604**, 323–329 (2022).
38. Duncan-Lowey, B. & Kranzusch, P. J. CBASS phage defense and evolution of antiviral nucleotide signaling. *Curr Opin Immunol* **74**, 156–163 (2022).
39. Haaber, J., Moineau, S., Fortier, L.-C. & Hammer, K. AbiV, a novel antiphage abortive infection mechanism on the chromosome of Lactococcus lactis subsp. cremoris MG1363. *Appl Environ Microbiol* **74**, 6528–37 (2008).
40. Matelska, D., Steczkiewicz, K. & Ginalski, K. Comprehensive classification of the PIN domain-like superfamily. *Nucleic Acids Res* **45**, 6995–7020 (2017).

41. Boyd, C. D. *et al.* Structural Features of the Pseudomonas fluorescens Biofilm Adhesin LapA Required for LapG-Dependent Cleavage, Biofilm Formation, and Cell Surface Localization. *J Bacteriol* **196**, 2775–2788 (2014).
42. Bull, J. J., Badgett, M. R., Springman, R. & Molineux, I. J. Genome properties and the limits of adaptation in bacteriophages. *Evolution (N Y)* **58**, 692 (2004).
43. Quinones-Olvera, N. *et al.* Diverse and abundant phages exploit conjugative plasmids. *Nat Commun* **15**, (2024).
44. Néron, B. *et al.* IntegronFinder 2.0: Identification and Analysis of Integrons across Bacteria, with a Focus on Antibiotic Resistance in Klebsiella. *Microorganisms* **10**, (2022).
45. Bouvier, M., Demarre, G. & Mazel, D. Integron cassette insertion: A recombination process involving a folded single strand substrate. *EMBO Journal* **24**, 4356–4367 (2005).
46. Loot, C., Ducos-Galand, M., Escudero, J. A., Bouvier, M. & Mazel, D. Replicative resolution of integron cassette insertion. *Nucleic Acids Res* **40**, 8361–8370 (2012).
47. Bouvier, M., Ducos-Galand, M., Loot, C., Bikard, D. & Mazel, D. Structural features of single-stranded integron cassette attC sites and their role in strand selection. *PLoS Genet* **5**, (2009).
48. Nivina, A., Escudero, J. A., Vit, C., Mazel, D. & Loot, C. Efficiency of integron cassette insertion in correct orientation is ensured by the interplay of the three unpaired features of attC recombination sites. *Nucleic Acids Res* **44**, 7792–7803 (2016).
49. MacDonald, D., Demarre, G., Bouvier, M., Mazel, D. & Gopaul, D. N. Structural basis for broad DNA-specificity in integron recombination. *Nature* **440**, 1157–1162 (2006).
50. Lacotte, Y., Ploy, M.-C. & Raherison, S. Class 1 integrons are low-cost structures in Escherichia coli. *ISME J* **11**, 1535–1544 (2017).
51. Carvalho, A. *et al.* The expression of integron arrays is shaped by the translation rate of cassettes. 2 3 ORCID. doi:10.1101/2024.03.26.586746.
52. Blanco, P. *et al.* Identification of Promoter Activity in Gene-Less Cassettes from Vibrionaceae Superintegrons. *Nucleic Acids Research. In press* (2023) doi:10.1101/2023.11.21.568050.
53. Barlow, R. S. & Gobius, K. S. Diverse class 2 integrons in bacteria from beef cattle sources. *Journal of Antimicrobial Chemotherapy* **58**, 1133–1138 (2006).
54. Rowe-Magnus, D. A., Guerout, A. M. & Mazel, D. Bacterial resistance evolution by recruitment of super-integron gene cassettes. *Mol Microbiol* **43**, 1657–1669 (2002).
55. Darracq, B. *et al.* Sedentary chromosomal integrons as biobanks of bacterial anti-phage defence systems. doi:10.1101/2024.07.02.601686.
56. Loot, C. *et al.* Integron cassettes integrate into bacterial genomes via widespread non-classical attG sites. *Nat Microbiol* **9**, 228–240 (2024).
57. Gao, L. *et al.* Diverse enzymatic activities mediate antiviral immunity in prokaryotes. *Science (1979)* **369**, 1077–1084 (2020).
58. Corbellino, M. *et al.* Eradication of a Multidrug-Resistant, Carbapenemase-Producing Klebsiella pneumoniae Isolate Following Oral and Intra-rectal Therapy With a Custom Made, Lytic Bacteriophage Preparation. *Clinical Infectious Diseases* **70**, 1998–2001 (2020).
59. Pirnay, J.-P. *et al.* Personalized bacteriophage therapy outcomes for 100 consecutive cases: a multicentre, multinational, retrospective observational study. *Nat Microbiol* **9**, 1434–1453 (2024).

60. Zhu, Y.-G. *et al.* Microbial mass movements. *Science (1979)* **357**, 1099–1100 (2017).
61. Gillings, M. *et al.* The evolution of class 1 integrons and the rise of antibiotic resistance. *J Bacteriol* **190**, 5095–5100 (2008).
62. Blanco, P. *et al.* Chromosomal Integrons are Genetically and Functionally Isolated Units of Genomes 2 3. doi:10.1101/2023.11.17.567518.
63. Song, L. *et al.* Phage Selective Pressure Reduces Virulence of Hypervirulent Klebsiella pneumoniae Through Mutation of the wzc Gene. *Front Microbiol* **12**, (2021).
64. Fujiki, J., Nakamura, K., Nakamura, T. & Iwano, H. Fitness Trade-Offs between Phage and Antibiotic Sensitivity in Phage-Resistant Variants: Molecular Action and Insights into Clinical Applications for Phage Therapy. *Int J Mol Sci* **24**, 15628 (2023).
65. Chan, B. K. *et al.* Phage selection restores antibiotic sensitivity in MDR Pseudomonas aeruginosa. *Sci Rep* **6**, 26717 (2016).
66. Alqurainy, N. *et al.* A widespread family of phage-inducible chromosomal islands only steals bacteriophage tails to spread in nature. *Cell Host Microbe* **31**, 69-82.e5 (2023).
67. Bonilla, N. *et al.* Phage on tap-a quick and efficient protocol for the preparation of bacteriophage laboratory stocks. *PeerJ* **4**, e2261 (2016).
68. Ács, N., Gambino, M. & Brøndsted, L. Bacteriophage Enumeration and Detection Methods. *Front Microbiol* **11**, 594868 (2020).
69. Tesson, F. *et al.* Systematic and quantitative view of the antiviral arsenal of prokaryotes. *Nat Commun* **13**, 2561 (2022).
70. van Kempen, M. *et al.* Fast and accurate protein structure search with Foldseek. *Nat Biotechnol* (2023) doi:10.1038/s41587-023-01773-0.
71. Mirdita, M. *et al.* ColabFold: making protein folding accessible to all. *Nat Methods* **19**, 679–682 (2022).
72. Yang, J. & Zhang, Y. Protein Structure and Function Prediction Using I-TASSER. *Curr Protoc Bioinformatics* **52**, (2015).
73. Gilchrist, C. L. M. & Chooi, Y.-H. clinker & clustermap.js: automatic generation of gene cluster comparison figures. *Bioinformatics* **37**, 2473–2475 (2021).
74. Bortolaia, V. *et al.* ResFinder 4.0 for predictions of phenotypes from genotypes. *Journal of Antimicrobial Chemotherapy* **75**, 3491–3500 (2020).
75. Carattoli, A. *et al. In Silico* Detection and Typing of Plasmids using PlasmidFinder and Plasmid Multilocus Sequence Typing. *Antimicrob Agents Chemother* **58**, 3895–3903 (2014).
76. Larsen, M. V. *et al.* Multilocus Sequence Typing of Total-Genome-Sequenced Bacteria. *J Clin Microbiol* **50**, 1355–1361 (2012).
77. Arndt, D. *et al.* PHASTER: a better, faster version of the PHAST phage search tool. *Nucleic Acids Res* **44**, W16–W21 (2016).
78. Avilan, L. Assembling Multiple Fragments: The Gibson Assembly. *Methods Mol Biol* **2633**, 45–53 (2023).
79. Ibarra-Chávez, R., Reboud, J., Penadés, J. R. & Cooper, J. M. Phage-Inducible Chromosomal Islands as a Diagnostic Platform to Capture and Detect Bacterial Pathogens. *Adv Sci (Weinh)* **10**, e2301643 (2023).
80. Biskri, L., Bouvier, M., Guérout, A. M., Boisnard, S. & Mazel, D. Comparative study of class 1 integron and Vibrio cholerae superintegron integrase activities. *J Bacteriol* **187**, 1740–1750 (2005).

947 81. DelaFuente, J., Rodriguez-Beltran, J. & San Millan, A. Methods to Study Fitness and
948 Compensatory Adaptation in Plasmid-Carrying Bacteria. *Methods in Molecular*
949 *Biology* **2075**, 371–382 (2020).
950